

A DFT and AIM analysis of the spin–spin couplings across the hydrogen bond in the 2-fluorobenzamide and related compounds

Ibon Alkorta,^{a*} José Elguero,^a Hans-Heinrich Limbach,^b Ilja G. Shenderovich,^b and Tammo Winkler^c



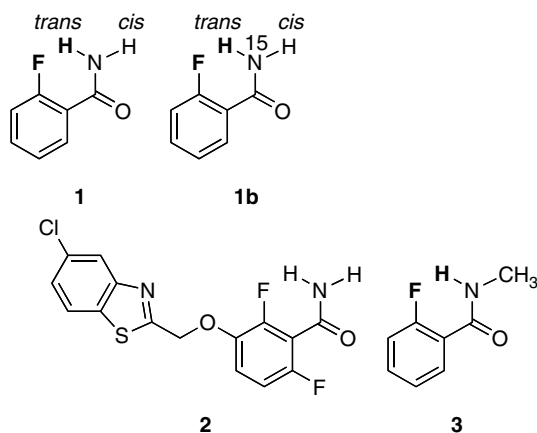
In 1975 a large number of coupling constants were measured in 2-fluorobenzamide labeled with ¹⁵N. Some of them were assigned to couplings through intramolecular N–H···F hydrogen bonds (HBs). These couplings change dramatically when CDCl₃ is replaced by DMSO-*d*₆. In this theoretical paper we provide density functional theory (DFT) calculations that justify the existence of a weak HB in the absence of solvent, while solvents that act as HB acceptors break down the intramolecular hydrogen bond (IMHB) of 2-fluorobenzamide. Atoms in molecules (AIM) analyses and Steiner-Limbach plots were used to analyze the structure of the compounds. Copyright © 2009 John Wiley & Sons, Ltd.

Supporting information may be found in the online version of this article.

Keywords: 2-fluorobenzamide; hydrogen bonds; solvent effects; spin-spin coupling constants; B3LYP/6-311++G**_s; AIM

Introduction

In 1974–1975, Fritz, Winkler and, in part Küng, published two papers describing the ¹H nuclear magnetic resonance (NMR) spectroscopy of 2-fluorobenzamide **1**.^[1,2] Particularly important is the second one because the molecule was ¹⁵N labeled (**1b**), thus allowing the measurement of many of its NMR properties (Table 1). The spectra were recorded at 100, 250 and 360 MHz and neither values nor assignments can be questioned. We should note that the important antibiotic PC190723 (**2**)^[3–5] shares part of the skeleton of **1**.



In 1993, Rae, Weigold, Contreras and Biekofsky^[6] studied **1** (without being aware of the previous results^[1,2]) as well as its *N*-methyl **3** and *N,N*-dimethyl derivatives by ¹H, ¹³C, ¹⁵N and ¹⁹F NMR spectroscopies (Table 2).

These authors^[6] established experimentally that the couplings were not through the bonds but through space involving an

intramolecular N–H···F hydrogen bond. The main argument was that 2-fluorobenzamide (**1**) and its *N*-methyl derivative (**3**) show spin–spin couplings between the aromatic fluorine and the nitrogen and carbon of the amide group, which are absent in the corresponding *N,N*-dimethylamide. But other possibilities remain such as a conformational change in the conformation of the *N,N*-dimethyl derivative.

In 1996 Forlani^[7] published a review on hydrogen bonding involving amino derivatives where the work of Rae *et al.*^[6] was cited but not those of Fritz and Winkler.^[1,2] Later on, some of us published 'A review with comprehensive data on experimental indirect scalar NMR spin–spin coupling constants across hydrogen bonds'^[8] where again^[6] was cited but not.^[1,2]

Two other things are relevant in this context. Schlosser *et al.*^[9] published in 1997 a paper on α -fluorocarboxamides, including **1** (citing again Ref. [6] but not Refs [1,2]) in where they stated that '... assuming strong intramolecular hydrogen bonding in two former cases (**1** and **3**). We consider this interpretation unwarranted' [note that never did Rae *et al.*^[6] suggested that the intramolecular hydrogen bond (IMHB) was strong]. The second aspect is related to a series of papers by Limbach *et al.*^[8,10] concerning the ^{2h}J(F–H···N) couplings (about –97 Hz), which are complementary to those studied here. Note that when the proton is transferred, in the first case a very unstable situation

* Correspondence to: Ibon Alkorta, Instituto de Química Médica, CSIC, Juan de la Cierva 3, E-28006 Madrid, Spain. E-mail: ibon@iqm.csic.es

^a Instituto de Química Médica, CSIC, Juan de la Cierva 3, E-28006 Madrid, Spain

^b Institut für Chemie and Biochemie, Takustrasse 3, Freie Universität Berlin, D-14195 Berlin, Germany

^c Solvias AG, Klybeckstrasse 191, 4057 Basel, Switzerland

Table 1. Chemical shifts (δ , ppm) and coupling constants (Hz) of compound **1b**^[2]

Solvent	Weight	δ_{NHc}	δ_{NHt}	$^1J_{\text{NHc}}$	$^1J_{\text{NHt}}$	$^2J_{\text{HcHt}}$	J_{NF}	J_{FHc}	J_{FHt}
CDCl ₃	5%	6.75	6.74	-89.0	-90.5	3.0	-7.0	+2.5	-11.5
CDCl ₃	1%	6.16	6.71						
DMSO- <i>d</i> ₆	5%	7.65	7.71	-88.5	-89.8	2.0	-3.2	< 1	2.4

Table 2. Chemical shifts (δ , ppm) and coupling constants (Hz) of compounds **1** and **3**^[6]

Compound	Solvent	$\delta^{15}\text{N}$	$\delta^{13}\text{C}(\text{CO})$	$\delta^{19}\text{F}$	J_{NF}	$^3J_{\text{CF}(\text{CO})}$	$^1J_{\text{CF}(\text{ipso})}$
1	CDCl ₃	-276.0	165.10	-113.24	-7.3 ^c	-2.5 ^c	-248.4 ^c
3 ^a	CDCl ₃	-275.9	163.88	-114.46	-7.4 ^c	-3.3 ^c	-246.0 ^c
3 ^a	CCl ₄	-272.7	-	-114.96	-6.7 ^c	-2.9 ^c	-246.0 ^c
3	Acetone- <i>d</i> ₆	-270.6	-	-114.14	-4.9 ^c	^b	-247.5 ^c
3	DMSO- <i>d</i> ₆	-267.0	-	-113.90	-2.8 ^c	^b	-248.7 ^c

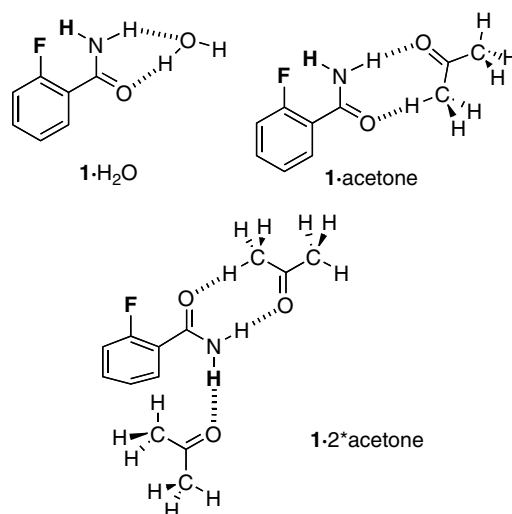
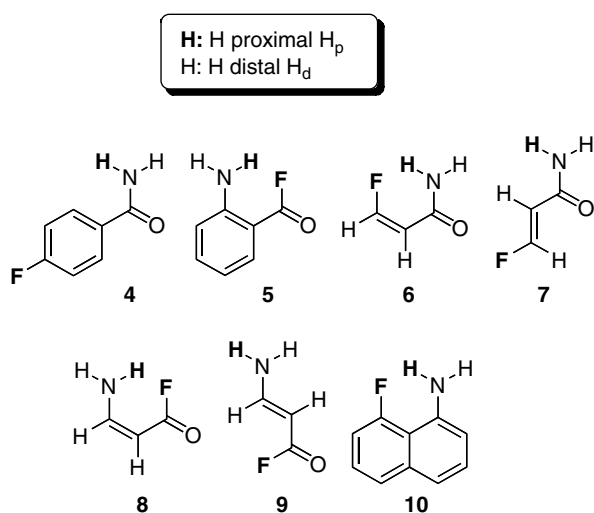
^a A $^6J(\text{F},\text{CH}_3)$ coupling of 1.2 Hz with the CH₃ was measured.

^b Not resolved.

^c We have changed the sign of these couplings to be consistent with the calculations (see Table 6)

(N⁻...H-F⁺) results while in the second one, the F⁻...H-N⁺, is stable when solvated. This could be related to the large difference in $^2hJ_{\text{FN}}$.

We decided to study theoretically compound **1** to see if its chemical shifts, coupling constants and solvent effects could be reproduced and to explore whether there is an IMHB or not. We have extended the calculations to other compounds, the *para* derivative **4**, an inverse structure, 2-aminobenzoyl fluoride (**5**), and to simplified models of **1**, **6** and **7**, and of **5**, **8** and **9**, as well as to 8-fluoronaphthalen-1-amine **10**, presenting similar motives; we changed the name of the amino hydrogen atoms from *trans/cis* to *proximal/distal* to cover all cases.



The geometry of the systems have been fully optimized at the B3LYP/6-311++G** level^[11,12] with the Gaussian 03 facilities.^[13] Frequency calculations have been carried out to confirm that the optimized structures correspond to energy minima. Absolute shieldings were calculated at the GIAO//B3LYP/6-311++G** level,^[11] which we are currently using in this kind of studies.^[14,15] Coupling constants were calculated at the B3LYP/6-311++G** level. The electron density has been analyzed using the Atoms in Molecules (AIM) methodology^[16] with the AIMPACK and AIM2000 programs.^[17,18]

Results and Discussion

Geometries and IR vibrations

We report on Table 3 the geometries of the F...H_p-N-H_d fragments.

One acetone molecule or one water molecule has little effect on the IMHB, while the second acetone molecule succeeds in breaking it down, producing a rotation of the amide group out of

Computational Details

We have calculated three complexes corresponding to different modes of solvation of **1**.

Table 3. Geometries (distances in Å, angles in °)

Compound	dF...H _p	dH _p -N	dN-H _d	Angle FH _p N
1	1.987	1.006	1.008	127.9
4	–	1.007	1.009	–
5	1.950	1.005	1.005	124.2
6	2.103	1.006	1.008	125.8
7	–	1.005	1.008	–
8	2.032	1.009	1.004	120.8
9	–	1.005	1.007	–
10	1.988	1.005	1.007	124.8
1 · 1 × H ₂ O	1.994	1.006	1.016	128.2
1 · 1 × acetone	1.993	1.005	1.018	129.0
1 · 2 × acetone	2.596	1.014	1.018	93.3

Table 4. NH₂ stretching vibrations (cm⁻¹)

Compd.	ν _s	ν _{as}	ν _s from Bellamy-Williams relationship ^[19]	diff.
1	3597	3731	3614	17
4	3585	3709	3595	10
5	3614	3734	3616	2
6	3595	3728	3611	16
7	3602	3732	3615	13
8	3595	3731	3614	19
9	3611	3733	3616	5
10	3604	3718	3602	-2
1 · H ₂ O	3486	3698	3585	99
1 · acetone	3448	3692	3580	132
1 · 2 × acetone	3441	3547	3453	12

the plane formed with the aromatic ring by 51.5°. Note also the importance of the benzene rings to constrain the IMHB to adopt a favorable geometry; compare the dF...H_p of **1/6** and **5/8** as well as the case of **10**.

The Bellamy-Williams relationship, displayed below, allows to analyze the properties of the NH₂.

$$\nu_s = 0.876 \nu_{as} + 345.5 \text{ (cm}^{-1}\text{)} \quad (1)$$

An examination of Table 4 shows that one water or acetone molecule strongly perturbs the stretching vibrations of the NH₂ group while two acetone molecules do not. The rest of compounds show small differences that are unrelated to the presence of IMHBs. This explains why Schlosser^[9] does not see hydrogen bonds (HBs) in infrared for **1**.

Chemical shifts

We will limit our discussion to compound **1** and its complexes **1** · H₂O, **1** · acetone and **1** · 2 × acetone and only to the F...H_p-N-H_d fragment (Table 5). We have transformed the absolute shields (σ, ppm) into chemical shifts (δ, ppm) using the following equations: δ¹H = 31.0 - 0.97 σ¹H; δ¹³C = 175.7 - 0.963 σ¹³C; δ¹⁵N = -154 - 0.98 σ¹⁵N; δ¹⁹F = 128.6 - 0.84 σ¹⁹F.^[14,15,20] At the same level of calculation, the absolute shieldings of the references are: 31.97 (¹H TMS), 184.75 (¹³C TMS), -154.43 (¹⁵N MeNO₂) and 153.70 (¹⁹F CFCl₃).

Table 5. Calculated chemical shifts (δ, ppm) of compound **1**

Compound	δNH _d	δNH _p	δ ¹⁵ N	δ ¹³ C(CO)	δ ¹⁹ F
1	4.88	6.39	-297.1	158.9	-113.3
1 · H ₂ O	7.46	6.56	-289.1	162.4	-113.5
1 · acetone	8.66	6.54	-287.9	160.3	-113.7
1 · 2 × acetone	8.26	8.01	-282.4	160.3	-109.9

Table 6. Calculated coupling constants (Hz); in the case of nitrogen they correspond to ¹⁵N

Compound	JFH _d	JFH _p	² JH _d H _p	JNF
1	+4.1	¹ hJ = -12.7	+5.0	² hJ = -7.4
4	-0.2	-0.4	+2.4	0.0
5	+7.2	¹ hJ = -14.9	+3.6	² hJ = -12.6
6	+1.9	-6.8	+4.8	-4.8
7	-0.5	-1.2	+3.9	+0.4
8	+1.1	¹ hJ = -10.8	+5.4	² hJ = -10.1
9	-1.2	-6.9	+4.4	-
10	+5.0	¹ hJ = -11.7	+0.7	² hJ = -10.1
1 · 1 × H ₂ O	+4.0	-12.3	+4.5	² hJ = -8.0
1 · 1 × acetone	+3.6	-12.2	+3.5	-7.0
1 · 2 × acetone	+0.2	+0.1	+2.8	+0.2

Compound	¹ JNH _d	¹ JNH _p	³ JCF(CO)	¹ JCF
1	-87.1	-89.1	-3.2	-299.0
4	-84.3 (<i>cis</i>)	-82.7 (<i>trans</i>)	-	-314.7
5	-90.9	-86.9	-	-379.7
6	-88.9	-87.8	0.4	-326.5
7	-89.5	-86.1	+16.3	-342.7
8	-91.6	-92.0	-10.1	-365.2
9	-93.2	-89.2	-	-374.9
10	-80.4	-84.6	-	-299.8
1 · H ₂ O	-89.0	-88.3	-3.2	-301.3
1 · acetone	-88.7	-86.4	-3.4	-299.8
1 · 2 × acetone	-86.0	-86.8	-1.4	-315.3

The experimental chemical shifts are reasonably well reproduced except δNH_d (δNH_c) (Tables 1 and 5) because the experimental value includes the effect of intermolecular HBs). More important, the sign of the solvent effects – solvent induced chemical shifts – is always described correctly by the calculations. For instance, the fact that the chemical shift of the proximal proton is less sensitive to dilution than that of the distal one (in CDCl₃) and that both protons become almost identical in DMSO-*d*₆ (here simulated by two acetone molecules) is also described by the calculations.

Coupling constants

We reported the calculated coupling constants in Table 6.

The agreement with the experimental data is reasonably good (compare Tables 1 and 2 with 6), taking into account that the values in CDCl₃ are compared with the isolated molecule and those in DMSO-*d*₆ with the complex **1** · 2 × acetone (Eqn 2).

$$\text{Experimental } J \text{ (Hz)} = (0.84 \pm 0.02) \text{ Calculated } J \text{ (Hz)}, \\ n = 18, r^2 = 0.992 \quad (2)$$

The calculated $^1J_{CF}$ are very sensitive to the nature of the carbon to which is linked (CH, CAr, CO) and to the C–F distance (see Supporting information). The 11 values of Table 6 can be adjusted to a multiple regression with an $r^2 = 0.992$ (Eqn 3).

$$^1J_{CF} \text{ (Hz)} = -(1412 \pm 162) + (20.4 \pm 3.0) \text{ CAr} \\ - (79.6 \pm 6.9) \text{ CO} + (8.0 \pm 1.2) dCF(\text{\AA}) \times 10^2 \quad (3)$$

Since $^1J_{CF}$ are always negative, this equation refers to the algebraic values showing that compared with CH, an aromatic ring increases the $^1J_{CF}$ coupling by 20.4 Hz and a CO decreases it by 79.6 Hz. When the CF distance increases by a hundredth of Å (for instance from 1.351 Å to 1.361 Å), the coupling increases 8.0 Hz. The IMHB affects dCF and this in turn modifies $^1J_{CF}$.

Atoms in molecules analysis

The topological analysis of the electron density using the AIM methodology shows the presence of a bond critical point between F and H_p (Figure 1 and Table 7).^[21–24]

No previous relationships between coupling constants through HBs and the corresponding values of ρ_{BCP} have been reported, although these are two important ways to characterize HBs. However, relationships between couplings and the value of the bond critical point in fluorine–fluorine through-space interactions have been found.^[20,25,26] Besides, Iranian authors described in two

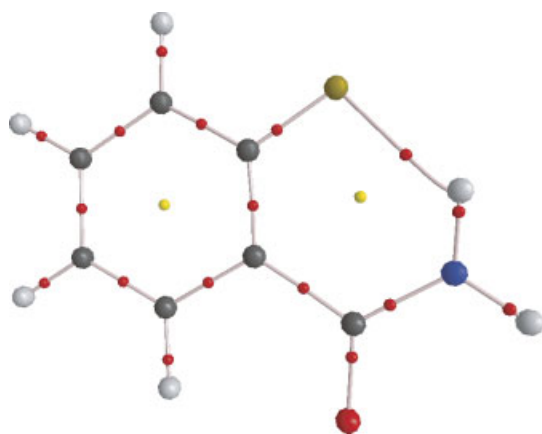
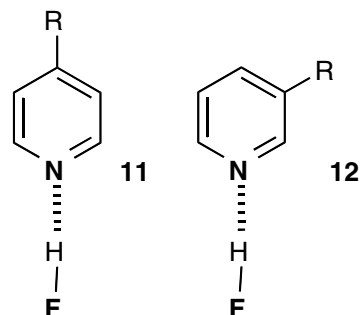


Figure 1. Bond critical points in compound **1** (the value for the HB is $\rho_{BCP} \times 10^2 = 2.17$).

Table 7. Results of the AIM calculations together with $^{2h}J_{NF}$			
Compound	$\rho_{BCP} \times 10^2 \text{ N} \cdots \text{F}$	Laplacian $\times 10^2 \text{ N} \cdots \text{F}$	$^{2h}J_{NF}$ (Hz)
1	2.17	9.24	–7.4
5	2.41	10.56	–12.6
6	1.69	6.93	–4.8
8	2.05	8.65	–10.1
10	2.21	9.54	–10.1
1 · H ₂ O	2.14	9.09	–8.0
1 · acetone	2.14	9.08	–7.0
HCN · · · HF	3.14	10.65	–22.2
N≡N · · · HF	1.64	6.74	–3.3
H₃N · · · HF	5.53	11.20	–36.7

papers calculated [MP2/6-311++G(d,p)] ρ_{BCP} ^[27] and calculated B3LYP/6-311++G(d,p) $^{2h}J_{NF}$ values^[28] for complexes of *para* **11** and *meta* substituted pyridines **12** with hydrogen fluoride, although they do not compare them nor their report $^1J_{FH}$ and $^1J_{NH}$. Using their 26 values, we have built up Figure 2. The regression line corresponds to Eqn 4.

$$^{2h}J_{NF} = (18.8 \pm 1.8) - (14.3 \pm 0.4) \rho_{BCP} \times 10^2, r^2 = 0.984 \quad (4)$$



That is, when ρ_{BCP} increases, $^{2h}J_{NF}$ decreases.

The point corresponding to **1** ($^{2h}J_{NF} = -7.4$ and $\rho_{BCP} \times 10^2 = 2.17$) is close to the weakest of pyridine/HF complexes (**12**, R = NH₃⁺, $^{2h}J_{NF} = -20.9$ and $\rho_{BCP} \times 10^2 = 2.56$) showing that **1** presents a very weak HB but consistent with its coupling constant. Figure 2 shows that $^{2h}J_{NF}$ depends only on the ρ_{BCP} of the hydrogen bond and not on the F–H · · · N or N–H · · · F character of the bond (the latter has already been proposed in Ref. 10b).

We have calculated $^1J_{FH}$ and $^1J_{NH}$ for the compounds of Table 7 plus three pyridine/HF complexes: **11a**, R = H, **11b**, R = O[–] and **11c**, R = NH₃⁺ (Table 8).

The data of Table 8 can be compared in several ways. For instance, in Figure 3 are reported the plots corresponding to the coupling constants and to the ρ_s :

Figure 3 (left) shows that along the N · · · H · · · F hydrogen bond, both coupling constants (FH and NH) change smoothly from 1J to

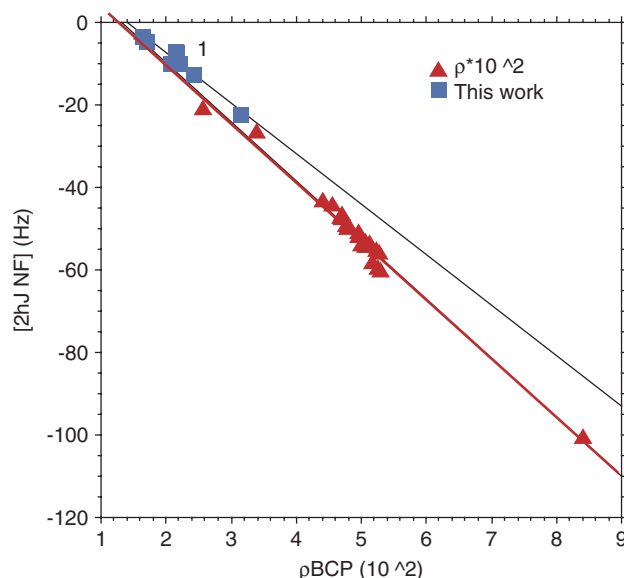


Figure 2. Plot of $^{2h}J_{NF}$ (Hz) versus ρ_{BCP} (10^2). Triangles, 26 pyridines/HF^[27,28]; squares, 10 values of Table 7.

Table 8. Results of the AIM calculations together with spin–spin coupling constants

Compound	$\rho_{\text{BCP}} \times 10^2$ HB	$\rho_{\text{BCP}} \times 10^2$ covalent	$^1J_{\text{FH}}$ (Hz)	$^1J_{\text{NH}}$ (Hz)
1	2.17	34.09	−12.7	−89.1
5	2.41	34.19	−14.9	−86.9
6	1.69	34.04	−6.8	−87.8
8	2.05	33.90	−10.8	−92.0
10	2.21	34.28	−11.7	−84.6
1 ·H ₂ O	2.14	34.14	−12.3	−88.3
1 ·acetone	2.14	34.17	−12.2	−86.4
11a	6.04	31.31	292.1	−0.5
11b	11.05	23.78	116.2	−16.5
11c	4.15	34.28	332.1	2.4
HCN ··· HF	3.14	34.80	364.8	3.4
N≡N ··· HF	1.64	36.33	364.9	2.4
H₃N ··· HF	5.53	31.76	298.0	1.6

$^1J_{\text{H}}$. Figure 3 (right) is a similar representation but now concerning bond critical points. In both figures, compound **11b** occupy a central position suggesting where similar compounds can be found. The fact that both figures are quite different is related to the complex relationships between J and ρ_{BCP} .^[20]

$$\rho_{\text{FH}} = (37.6 \pm 0.4) - (1.04 \pm 0.02)\rho_{\text{NH}}, \quad n = 13, r^2 = 0.998 \quad (5)$$

Steiner-Limbach analysis

It has been known for some time that coupling constants across hydrogen bonds are correlated with the hydrogen bond geometries. In order to describe this correlation, one of us has used Pauling's valence bond orders.^[29,30]

$$p_1 = \exp\{-(r_1 - r_1^0)/b_1\}, \quad p_2 = \exp\{-(r_2 - r_2^0)/b_2\},$$

with $p_1 + p_2 = 1$ (6)

In Eqn (6), r_1^0 corresponds to the distance in free AH and r_2^0 in free HB. b_1 and b_2 are empirical parameters describing the decrease of the valence bond order with increasing distances. Instead of the average distances r_1 and r_2 their combinations $q_1 = 1/2(r_1 - r_2)$ and $q_2 = r_1 + r_2$ have been shown to be very useful. In the case of linear hydrogen bonds where the average hydrogen bond angle α

is about 180° , q_1 corresponds to the deviation of hydrogen nucleus from the hydrogen bond center and q_2 to the A···B distance.

Equation (6) predicts that this distance decreases when the proton is shifted from A towards the hydrogen bond center, and then increases again when the proton has crossed the center as illustrated in Figure 4(a). The solid line was calculated using the distance parameters listed in Table 9. These parameters were established by some of us previously by *ab initio* calculations of $\text{FH} \cdots \text{NH}_3$, where H was shifted from F to N by increasing the strength of a homogeneous electric field.^[31] We note that all hydrogen bond geometries of the systems calculated in this work, represented by open squares are well located on the same solid correlation line. The open circles refer to the geometries of complexes of 2,4,6-trimethylpyridine (collidine) complexes with HF in $\text{CDF}_3/\text{CDF}_2\text{Cl}$ mixtures,^[10,32] and of fluorobenzamide^[2] in $\text{DMSO}-d_6$ and CDCl_3 derived from the experimental coupling constants as described below.

The solid lines in Figure 4(b)–(d) represent the correlation curves $^1J_{\text{FH}} = f(q_1)$, $^1J_{\text{HN}} = f(q_1)$ and $^2J_{\text{FN}} = f(q_1)$. Roughly, for a hydrogen bond AHB, when the A–H distance is increased and H shifted towards B, the coupling constant $^1J_{\text{AH}}$ decreases. After H has passed the H-bond center, this coupling constant is often labeled as $^1J_{\text{AH}}$. The coupling goes then to zero, changes sign and only at large A···H distances the coupling really vanishes.^[29,33] This feature is well pronounced for $\text{F} \cdots \text{H}$, whereas the effect is much smaller for $\text{H} \cdots \text{N}$. On the other hand, $^2J_{\text{AB}} = f(q_1)$ exhibits a typical bell-shaped curve with a maximum around $q_1 = 0$, where the values vanish at large A···B distances.

The solid lines were calculated using the following equations proposed previously.^[10,29]

$$^1J_{\text{FH}} = ^1J_{\text{FH}}^0 p_{\text{FH}} - 2^{m+n} \Delta J_{\text{FHN}} p_{\text{FH}}^m p_{\text{HN}}^n \quad (7)$$

$$^1J_{\text{HN}} = ^1J_{\text{HN}}^0 p_{\text{HN}} - 2^{m+n} \Delta J_{\text{NHF}} p_{\text{FH}}^n p_{\text{HN}}^m \quad (8)$$

$$^2J_{\text{FN}} = ^2J_{\text{FN}}^0 2^{m+n} p_{\text{FH}} p_{\text{HN}}^n \quad (9)$$

The parameters of these equations used in Figure 4 are included in Table 9 while in Table 10 are reported the data points used to construct Figures 4 and 5.

These parameters are still tentative as they depend on the body of data points available. As a number of new data points are included here the parameters differ somewhat from those used previously only for the collidine–HF complexes.^[10b] Nevertheless, the calculated solid lines fit the experimental data points in Figure 4 in a very satisfactory way, in view of the fact that only hydrogen

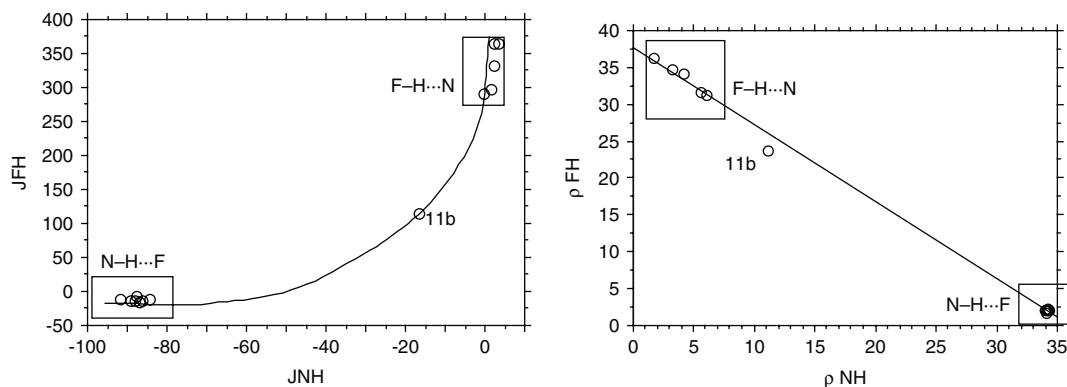


Figure 3. Left side: Plot of $^1J_{\text{FH}}$ (Hz) versus $^1J_{\text{NH}}$ (Hz). Right side: Plot of ρ_{BCP} (FH) versus ρ_{BCP} (NH) [the straight line corresponds to (Eqn 5)].

Table 9. Parameters of the FHN-hydrogen bond correlations in Figures 4 and 5

b_{FH}	r_{FH}°	b_{HN}	r_{HN}°	${}^1J_{\text{FH}}^{\circ}$	ΔJ_{FHN}	m	n	${}^1J_{\text{HN}}^{\circ}$	ΔJ_{NHF}	m	n	${}^2J_{\text{FN}}^{\circ}$	m	n
0.36 ^a	0.897 ^a	0.385 ^a	0.992 ^a	540 ^b	160 ^b	1 ^b	2.2 ^b	-95 ^c	15 ^c	2.4 ^c	1 ^c	-110 ^d	1.5 ^d	1.5 ^{dc}

Distances in Å, coupling constants in Hz.
^a Equation (6).
^b Equation (7).
^c Equation (8).
^d Equation (9).

Table 10. Data points used to construct Figures 4 and 5 (without the collidine HF complexes)

Compound	r_{FH}	r_{HN}	J_{FH}	J_{HN}	J_{NF}	q_1	q_2
1	1.987	1.006	-12.7	-89.1	-7.4	0.4905	2.993
5	1.95	1.005	-14.9	-86.9	-12.6	0.4725	2.955
6	2.103	1.006	-6.8	-87.8	-4.8	0.5485	3.109
8	2.032	1.009	-10.8	-92	-10.1	0.5115	3.041
10	1.988	1.005	-11.7	-84.6	-10.1	0.4915	2.993
2 · H₂O	1.994	1.006	-12.3	-88.3	-8.0	0.494	3
2-acetone	1.993	1.005	-12.2	-86.4	-7.0	0.494	2.998
11a	0.965	1.639	292.1	-0.5	-52.16	-0.337	2.604
11b	1.049	1.409	116.2	-16.5	-100.82	-0.18	2.458
11c	0.941	1.777	332.1	2.4	-26.83	-0.418	2.718
HCN · HF	0.936	1.837	364.8	3.4	-22.24	-0.4505	2.773
NN · HF	0.926	2.075	364.9	2.4	-3.29	-0.5745	3.001
H₃N · HF	0.961	1.674	298.0	1.6	-36.73	-0.3565	2.635
2 · 2 × acetone	2.596	1.014	0.1	-86.8	0.2	0.791	3.61
1b CDCl₃	2	1	-11.5	-90.5	-7.0	0.5	3
1b DMSO	2	1	-2.4	-89.8	-3.2	0.6	3.2

bond geometries are taken into account but no other chemical and structural effects.

${}^1J_{\text{FH}}^{\circ}$ represents the coupling constant of free HF at the equilibrium configuration. Here, we calculated at the B3LYP/6-311++G** level a value of 351.7 Hz. At higher levels of calculation, values of up to 510 Hz have been calculated.^[34,35] The experimental value at the equilibrium configuration is 540 Hz.^[36] We adopted here the latter value. This means, however, also that all ${}^1J_{\text{FH}}$ values calculated at the B3LYP/6-311++G** level are too small, and have, thus to be scaled in an appropriate way, which is most important for the large values at $q_1 < 0$. At first sight, a scaling factor of 540/350 seemed to be appropriate. However, this factor was too large, and in order to place the calculated data points in Figure 4(b) on the solid correlation line we had to use a factor of 540/400.

The parameter ΔJ_{FHN} represents the excess decrease of ${}^1J_{\text{FH}}$ as compared to ${}^1J_{\text{FH}}^{\circ}/2$ at a FH bond order of 1/2. This value determines where ${}^1J_{\text{FH}}$ goes to zero as well as the maximum negative value when H has passed the H-bond center.

The value of ${}^1J_{\text{HN}}^{\circ}$ was estimated as follows. First, calculations of isolated protonated pyridines at the B3LYP/6-311++G** level gave values between -91 and -94 Hz. Therefore, we adopted a value of -95 Hz. We note that this value is valid only for sp² hybridized nitrogen atoms, as the collidine-HF complexes as well as fluorobenzamide. However, it is larger for sp-hybridized nitrogen atoms^[29] such as NCN · HF, N≡N · HF and for sp³ nitrogen atoms such as H₃N · HF. However, in these complexes H was calculated to be close to fluorine, and the different correlation

lines ${}^1J_{\text{HN}} = f(q_1)$ of the different types of nitrogen atoms coincide in this region. Because of the gyromagnetic ratio of ¹⁵N, ${}^1J_{\text{HN}}$ is negative for small NH distances. However, as in the FH case but to a smaller extent, we find here a sign change at larger N · · · H distance which is well reproduced by the value of ΔJ_{NHF} .

The correlation ${}^2J_{\text{FN}} = f(q_1)$ depicted in Figure 4(d) is well reproduced by Eqn (4). Here, the problem was to estimate the maximum value $-{}^2J_{\text{FN}}^{\circ}$ for the shortest hydrogen bond. Previously,^[10b] we had taken the experimental value of $-{}^2J_{\text{FN}} = 96$ Hz found for collidine-HF as maximum value. Here, the calculations indicate slightly larger values for substituted pyridine · · · HF complexes which lead us to increase $-{}^2J_{\text{FN}}^{\circ}$ to 110 Hz in order to satisfy the equation corresponding to all data in Figure 4(d). The smaller experimental values can be explained in terms of quantum zero point vibrational effects as proposed previously for NHN^[37] and OHN^[38] systems. Because of the width of the zero-point vibration of the proton, the real N · · · F distances are larger in the strong short hydrogen bond regime than the equilibrium distances.^[30]

Finally, we have adapted slightly the exponents in Eqns (2) to (4). These exponents influence the form of the correlation lines. This is especially evident in the case of ${}^2J_{\text{FN}} = f(q_1)$, where an increase of m and n leads to a narrowing of the bell-shaped correlation curve.

In order to estimate the hydrogen bond geometries of the systems for which coupling constants were obtained experimentally we proceeded as described before.^[10] We searched optically for the best value of q_1 where the set of experimental values ${}^1J_{\text{FH}}$, ${}^1J_{\text{HN}}$ and ${}^2J_{\text{FN}}$ represented by the open circles satisfied the solid hydrogen bond correlation lines. In this way, we determined also the value of q_2 and hence the values of $r_1 = r_{\text{FH}}$ and $r_2 = r_{\text{HN}}$. For the collidine-HF complexes these values were the same as reported previously.^[10b] For fluorobenzamide in CDCl₃ we find the values of $r_{\text{FH}} = 2.0$ Å and $r_{\text{HN}} = 1.0$ Å which compare well with the calculated values of 1.987 Å and 1.006 Å. These results demonstrate the power of the analysis in Figure 4.

In Figure 5 we have prepared a graph where ${}^1J_{\text{FH}}$ and ${}^2J_{\text{FN}}$ are plotted as a function of ${}^1J_{\text{HN}}$. As was discussed before,^[29] such a plot can be useful for the experimentalist when calculated coupling constants are not yet available. The solid lines were calculated using Eqns (2) to (4); they reproduce the calculated and experimental data in a very satisfactory way. The non-monotonous solid lines illustrate well the sign changes of both ${}^1J_{\text{HN}}$.

Conclusions

The main conclusions of the present study are:

- Along the N · · · H · · · F hydrogen bond there is a continuity of situations from the proton close to the N atom to the proton close to the F atom, although the central positions are empty (no molecules with the proton in the middle or near the middle).

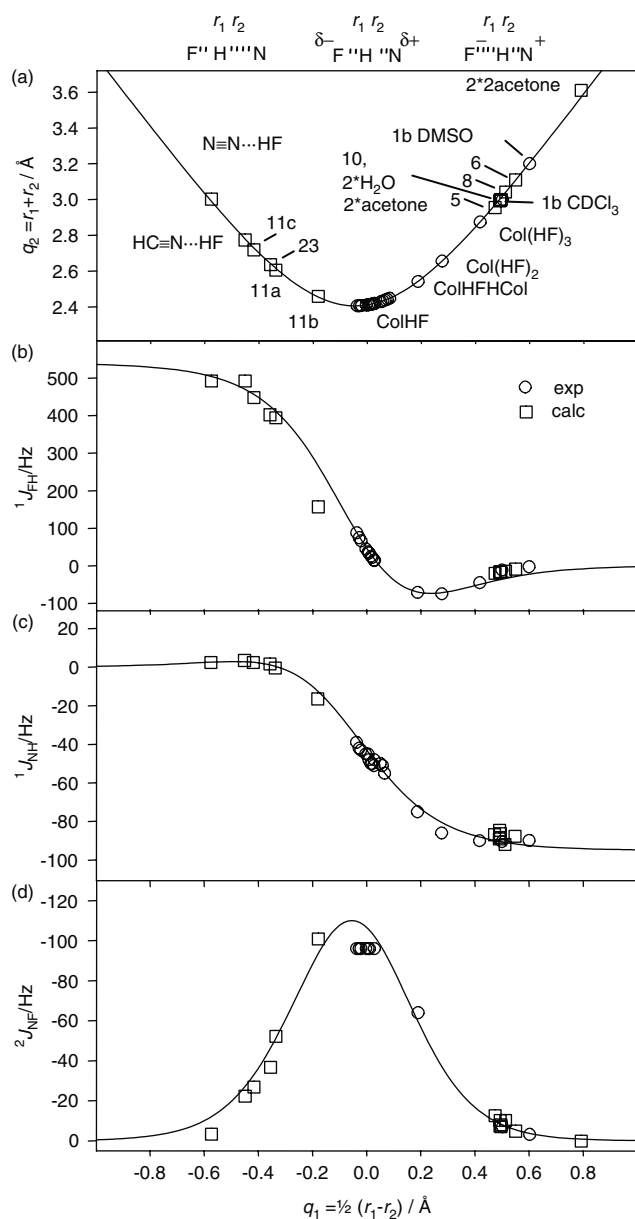


Figure 4. FHN hydrogen bond correlations. (a) Geometric correlation q_2 as a function of q_1 . (b), (c) and (d) correlations of the coupling constants $^1J_{FH}$, $^1J_{NH}$ and $^2J_{NF}$ as a function of q_1 . The solid lines are calculated according to the valence bond model as described in the text.

- (ii) Compound **1** presents an IMHB in chloroform that disappears in DMSO due to the formation of intermolecular HBs with the solvent.
- (iii) Other compounds, such as **5** and **10** should show $^2J_{NF}$ couplings.
- (iv) Bader analysis provides a useful description of HBs that match NMR spin–spin coupling constants.
- (v) Figures 4 and 5 illustrate the use of NMR hydrogen bond correlations, which allow one to estimate average hydrogen bond geometries in solution.

Acknowledgements

This work has been financed by the Spanish MEC (CTQ2007-62113 and CTQ2007-61901/BQU) and Comunidad Autónoma de Madrid

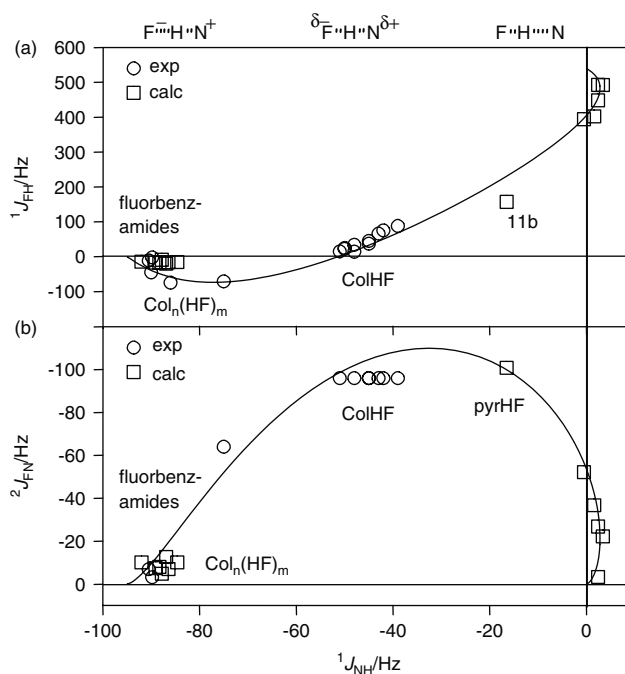


Figure 5. Experimental and calculated constants of FHN hydrogen bonds. (a) $^1J_{FH}$ and (b) $^2J_{FN}$ as a function of $^1J_{NH}$. The solid lines are calculated according to the valence bond model as described in the text.

(Project MADRISOLAR, ref. S-0505/PPQ/0225). HHL and IGS thank Dr. N. S. Golubev and Prof. G. S. Denisov, St. Petersburg, and Dr. P. Tolstoy, St. Petersburg and Berlin for stimulating discussions. We also acknowledge the financial support of the Deutsche Forschungsgemeinschaft, Bonn and the Fonds der Chemischen Industrie, Frankfurt.

Supporting information

Supporting information may be found in the online version of this article.

References

- [1] H. Fritz, T. Winkler, *Helv. Chim. Acta* **1974**, *57*, 836.
- [2] H. Fritz, T. Winkler, W. Küng, *Helv. Chim. Acta* **1975**, *58*, 1822.
- [3] D. Payne, *Science* **2008**, *321*, 1644.
- [4] T. Hiratsuka, K. Furihata, J. Ishikawa, H. Yamashita, N. Itoh, H. Seto, T. Dairi, *Science* **2008**, *321*, 1670.
- [5] D. Haydon, N. R. Sokes, R. Ure, G. Galbraith, J. M. Bennett, D. R. Brown, P. J. Baker, V. V. Barynin, D. W. Rice, S. E. Sedelnikova, J. R. Heal, J. M. Sheridan, S. T. Aiwale, P. K. Chauhan, A. Srivastava, A. Taneja, I. Collins, J. Errington, L. G. Czaplowski, *Science* **2008**, *321*, 1673.
- [6] I. D. Rae, J. A. Weigold, R. H. Contreras, R. R. Biekofsky, *Magn. Reson. Chem.* **1993**, *31*, 836.
- [7] L. Forlani, Hydrogen bonding and complex formation involving compounds with amino, nitroso and nitro groups, in *The Chemistry of Amino, Nitroso, Nitro and Related Groups*, Supplement F2, Part 1, (Ed.: S. Patai), John Wiley & Sons, New York, **1996**, p 438, Chapt. 10.
- [8] I. Alkorta, J. Elguero, G. S. Denisov, *Magn. Reson. Chem.* **2008**, *46*, 599.
- [9] D. Michel, M. Witschard, M. Schlosser, *Liebigs Ann./Recueil* **1997**, 517.
- [10] (a) N. S. Golubev, I. G. Shenderovich, S. N. Smirnov, G. S. Denisov, H. H. Limbach, *Chem. Eur. J.* **1999**, *5*, 492; (b) I. G. Shenderovich, P. Tolstoy, N. S. Golubev, S. N. Smirnov, G. S. Denisov, H. H. Limbach, *J. Am. Chem. Soc.* **2003**, *125*, 11710.

- [11] (a) A. D. Becke, *J. Chem. Phys.* **1993**, *98*, 5648; (b) C. Lee, W. Yang, R. G. Parr, *Phys. Rev. A* **1988**, *37*, 785.
- [12] M. J. Frisch, J. A. Pople, R. Krishnan, J. S. Binkley, *J. Chem. Phys.* **1984**, *80*, 3265.
- [13] M. J. Frisch, G. W. Trucks, H. B. Schlegel, G. E. Scuseria, M. A. Robb, J. R. Cheeseman, J. A. Montgomery Jr, T. Vreven, K. N. Kudin, J. C. Burant, J. M. Millam, S. S. Iyengar, J. Tomasi, V. Barone, B. Mennucci, M. Cossi, G. Scalmani, N. Rega, G. A. Petersson, H. Nakatsuji, M. Hada, M. Ehara, K. Toyota, R. Fukuda, J. Hasegawa, M. Ishida, T. Nakajima, Y. Honda, O. Kitao, H. Nakai, M. Klene, X. Li, J. E. Knox, H. P. Hratchian, J. B. Cross, C. Adao, J. Jaramillo, R. Gomperts, R. E. Stratmann, O. Yazyev, A. J. Austin, R. Cammi, C. Pomelli, J. W. Ochterski, P. Y. Ayala, K. Morokuma, G. A. Voth, P. Salvador, J. J. Dannenberg, V. G. Zakrzewski, S. Dapprich, A. D. Daniels, M. C. Strain, O. Farkas, D. K. Malick, A. D. Rabuck, K. Raghavachari, J. B. Foresman, J. V. Ortiz, Q. Cui, A. G. Baboul, S. Clifford, J. Cioslowski, B. B. Stefanov, G. Liu, A. Liashenko, P. Piskorz, I. Komaromi, R. L. Martin, D. J. Fox, T. Keith, M. A. Al-Laham, C. Y. Peng, A. Nanayakkara, M. Challacombe, P. M. W. Gill, B. Johnson, W. Chen, M. W. Wong, C. Gonzalez, J. A. Pople, *Gaussian 03*, Gaussian: Pittsburgh, **2003**.
- [14] F. Blanco, I. Alkorta, J. Elguero, *Magn. Reson. Chem.* **2007**, *45*, 797.
- [15] A. M. S. Silva, R. M. S. Sousa, M. L. Jimeno, F. Blanco, I. Alkorta, J. Elguero, *Magn. Reson. Chem.* **2007**, *45*, 859.
- [16] (a) R. F. W. Bader, *Acc. Chem. Res.* **1985**, *18*, 9; (b) R. F. W. Bader, *Chem. Rev.* **1991**, *91*, 893; (c) R. F. W. Bader, *Atoms in Molecules, A Quantum Theory*, Oxford University Press: Oxford, **1990**; (d) R. F. W. Bader, *J. Phys. Chem. A* **1998**, *102*, 7314.
- [17] F. W. Bieger-König, R. F. W. Bader, T. H. Tang, *J. Comput. Chem.* **1982**, *3*, 317.
- [18] F. Biegler-König, J. Schönbohm, *AIM2000, Version 2.0*, Bielefeld, **2002**.
- [19] L. J. Bellamy, *Advances in Infrared Group Frequencies*, Methuen: London, **1969**, p. 110, 280.
- [20] I. Alkorta, J. Elguero, *Struct. Chem.* **2004**, *15*, 117.
- [21] I. Mata, I. Alkorta, E. Espinosa, E. Molins, J. Elguero, in *The Quantum Theory of Atoms in Molecules* (Eds: C. F. Matta, R. J. Boyd), Wiley-VCH: Weinheim, **2007**, p 425, Chapt. 16.
- [22] A. M. Pendás, E. Francisco, M. A. Blanco, C. Gatti, *Chem. Eur. J.* **2007**, *13*, 9362.
- [23] J. J. Novoa, E. D'Oria, *Engineering of Crystalline Materials Properties*, Springer: Netherlands, **2008**.
- [24] I. Alkorta, J. Elguero, in *Aromaticity in Heterocyclic Compounds* (Eds: T. M. Krygowski, M. K. Cyranski), Springer, Berlin, **2009**, pp. 155.
- [25] N. Castillo, C. F. Matta, R. J. Boyd, *J. Chem. Inf. Model.* **2005**, *45*, 354.
- [26] C. F. Matta, N. Castillo, R. J. Boyd, *J. Phys. Chem. A* **2005**, *109*, 3669.
- [27] A. Ebrahimi, M. Habibi, H. R. Masoodi, *Chem. Phys.* **2007**, *340*, 85.
- [28] A. Ebrahimi, M. Habibi, H. R. Masoodi, A. R. Gholipour, *Chem. Phys.* **2009**, *355*, 67.
- [29] H. Benedict, I. G. Shenderovich, O. L. Malkina, V. G. Malkin, G. S. Denisov, N. S. Golubev, H. H. Limbach, *J. Am. Chem. Soc.* **2000**, *122*, 1979.
- [30] H. H. Limbach, G. S. Denisov, N. S. Golubev, in *Isotope Effects in Chemistry and Biology, Hydrogen Bond Isotope Effects Studied by NMR* (Eds: A. Kohen, H. H. Limbach), Taylor & Francis: Boca Raton, **2005**, pp 193, Chapt. 7.
- [31] M. Ramos, I. Alkorta, J. Elguero, N. S. Golubev, G. S. Denisov, H. Benedict, H. H. Limbach, *J. Phys. Chem.* **1997**, *A101*, 9791.
- [32] I. G. Shenderovich, A. P. Burtsev, G. S. Denisov, N. S. Golubev, H. H. Limbach, *Magn. Reson. Chem.* **2001**, *39*, S91.
- [33] I. G. Shenderovich, S. Smirnov, G. S. Denisov, V. Gindin, N. S. Golubev, A. Dunger, R. Reibke, S. Kirpekar, O. L. Malkina, H. H. Limbach, *Ber. Bunsen. Phys. Chem.* **1998**, *102*, 422.
- [34] P. O. Åstrand, K. Ruud, K. V. Mikkelsen, T. Helgaker, *J. Chem. Phys.* **1999**, *110*, 9463.
- [35] J. E. Del Bene, J. Elguero, *Solid State NMR* **2008**, *34*, 86.
- [36] S. M. Bass, R. L. DeLeon, J. S. Muentzer, *J. Chem. Phys.* **1987**, *86*, 4305.
- [37] H. H. Limbach, M. Pietrzak, H. Benedict, P. M. Tolstoy, N. S. Golubev, G. S. Denisov, *J. Mol. Struct.* **2004**, *706*, 115.
- [38] H. H. Limbach, M. Pietrzak, S. Sharif, P. M. Tolstoy, I. G. Shenderovich, S. N. Smirnov, N. S. Golubev, G. S. Denisov, *Chem. Eur. J.* **2004**, *10*, 5195.